Available online at www.sciencedirect.com
SCIENCE DIRECT®
Journal of Power Sources 124 (2003) 321–329
JOURNAL OF POWER SOURCES
www.elsevier.com/locate/jpowsour

Investigation of electrochemical double-layer (ECDL) capacitors electrodes based on carbon nanotubes and activated carbon materials

Ch. Emmenegger[a,*], Ph. Mauron[a], P. Sudan[a], P. Wenger[a], V. Hermann[b], R. Gallay[b], A. Züttel[a]

[a] *Physics Institute, University of Fribourg, Pérolles, CH-1700 Fribourg, Switzerland*
[b] *Montena Components, CH-1728 Rossens, Switzerland*

Received 12 December 2002; received in revised form 14 April 2003; accepted 5 May 2003

Abstract

The carbon nanotubes (CNT) show promising electrochemical characteristics particularly for electrochemical energy storage. The electrochemical double-layer (ECDL) capacitor is a new type of capacitor with features intermediate between those of a battery and a conventional capacitor. ECDL capacitors have been made using various types of CNT and activated carbon (a-C) as electrode material. The specific capacitance per surface area of the electrodes depends on the thickness and the specific surface area of the active material. The CNT electrodes show a specific capacitance from 0.8 and 280 mF cm^{-2} and 8 to 16 F cm^{-3}, respectively. Increasing the mass density also helps to increase the capacitance. Commercially available activated carbon (a-C) electrodes were also tested in order to study their specific capacitance as a function of their physical properties. The various a-C electrodes have specific capacitance per surface area ranging from 0.4 to 3.1 F cm^{-2} and an average specific capacitance per volume of 40 F cm^{-3} due to their larger mass density.

Keywords: Carbon nanotubes; Specific capacitance; ECDL capacitor; Activated carbon; Supercapacitors

1. Introduction

There have been considerable efforts to develop new methods of efficient energy storage. This application requires a high specific power from approximately 1–10 kW kg^{-1} [1], and a specific energy density of 0.5–10 Wh kg^{-1} [2]. The most common storage system of electrical energy is the battery. However, the cycle life and power (below 100 W kg^{-1}) [1] limit the use of batteries for many mobile applications. Batteries are useful for storage over long-time application (>100 s), while conventional capacitors [3] are useful for short-time storage (<0.01 s). Conventional capacitors provide a high power (>103 kW kg^{-1}) and a long cycle life, but with a small energy density (about 70 mW kg^{-1}) [1]. The capacitance C of the conventional capacitors is given by Eq. (1):

$$C = \frac{\varepsilon_o \varepsilon_r A_E}{d} \quad (1)$$

where A_E is the geometric surface area of the electrode, ε_o the permittivity of the vacuum, ε_r the relative permittivity of the dielectric material and d is the distance between the two electrodes. The amount of electrical energy (Wh kg^{-1}) stored in the polarised dielectric material [4] is given by Eq. (2):

$$W = \frac{1}{2}\frac{CU^2}{m_{act}} \quad (2)$$

where U is the working voltage and m_{act} is the amount of active material. Conventional capacitors have the advantage of high working voltage. However, their specific energy capacity is limited by the breakdown field (V μm^{-1}) of their dielectric material. Overall, conventional capacitors do not have a large enough energy storage capacity for applications where significant energy is needed. The electrochemical double-layer capacitor (ECDL) [5] has been developed for these cases which need a large energy density (Wh kg^{-1}), high power density (W kg^{-1}) and long cycle life (>100,000). The ECDL capacitor is a new type of capacitor offering new features intermediate those of a battery and a conventional capacitor [2].

The ECDL capacitor consists of two electrodes that are immersed in an electrolyte with a separator between them (Fig. 1, top). The electrode consists of a current collector in contact with the active material. In ECDL capacitors, the energy storage arises mainly from the separation of electronic

* Corresponding author. Tel.: +41-26-300-9101; fax: +41-26-300-9747.
E-mail address: cemmenegger@asulab.ch (Ch. Emmenegger).

0378-7753/$ – see front matter © 2003 Elsevier B.V. All rights reserved.
doi:10.1016/S0378-7753(03)00590-1

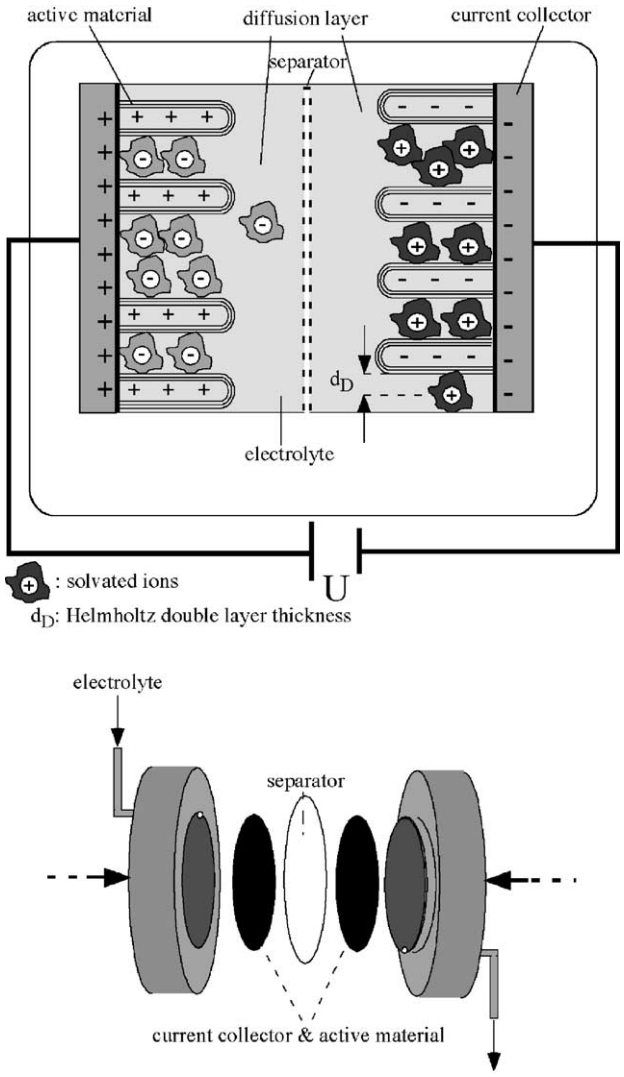

Fig. 1. Top: sketch of the electrochemical double-layer capacitor based on well-aligned MWNT, bottom: schematic view of the ECDL test cell.

and ionic charges at the interface between high-area electrode material and the electrolyte solution (Fig. 1, top). In the ECDL, this charge separation d distance is reduced to the Helmholtz double-layer d_D thickness, which is defined as half the diameter of the adsorbed solvated ions at the electrode/solution interface (Fig. 1, top) [6].

The electrode material should be electrochemically inert in the working potential, which is limited by the decomposition potential of the electrolyte [7]. Carbon materials such as carbon nanotubes (CNT) [8] and activated carbon (a-C) are very attractive as electrode materials in the ECDL capacitors [9] due to their large specific surface area and low mass density. Indeed, multiwalled (MWNT) and single walled (SWNT) nanotubes are well adapted to allow the electrolyte accessibility because of their morphology, high BET (100–1315 $m^2\,g^{-1}$) specific surface area [10] and good mechanical properties [11].

A comparison of the performance of the three electricity storage systems in Table 1 shows that the ECDL capacitors using CNT are a remarkable compromise between the batteries and the conventional capacitors [12]. Recent studies of ECDL capacitors using CNT [13–19] showed performance comparable to those using a-C [20,21] (Table 2).

Table 1
Comparison values between a conventional capacitor, an ECDL capacitor based on CNT and a Ni-Cd battery

	Conventional capacitor	ECDL capacitor based on CNT	Battery Ni-Cd
Surface electrode (cm^2)	1	1	–
Electrolyte	–	Organic	Aqueous
Density ($g\,cm^{-3}$)	0.9×10^{-3} (*separator*)	0.4	–
Specific surface area ($m^2\,g^{-1}$)	–	100	–
Active material thickness (μm)	10	30	–
Dielectric constant, ε_r	2	40	–
Diameter of ions (nm)	–	1.2	–
Double-layer capacitor ($\mu F\,cm^{-2}$)	4.67×10^{-6}	62	–
Total surface area (cm^2)	1	1147	–
Capacitance ($mF\,cm^{-2}$)	4.67×10^{-9}	71	–
Working voltage (V)	1000	2.5	1.2
Power density (kW kg)	2.7 E10	260	<0.1
Energy density (Wh kg)	0.072	15	225
Time application (s)	<0.01	0.1–1	>100
Cycle life	>10000	>100000	1000

Table 2
Recent results of the ECDL capacitors based on CNT and a-C

Authors	Active material	BET surface area ($m^2\,g^{-1}$)	C_{sp} ($F\,g^{-1}$)	C_{sp} ($F\,cm^{-2}$)	Electrolyte
Niu et al. [13]	dc-arc MWNT	430	49–102	0.08–0.17	Aqueous
An et al. [14]	dc-arc MWNT	357	71–180	0.3–0.8	Organic
Ma et al. [15]	CVD MWNT	120	15–25	–	Aqueous
Chen et al. [16]	CVD MWNT	–	115.7	0.06	Aqueous
E. Frackowiak [17]	SWNT *Rice Uni.*	410	18–40	0.012–0.06	Aqueous
	CVD-MWNT	200–400	36–172	0.054–0.26	Aqueous
S. Shiraishi [18]	dc-arc SWNTs	500	45	0.00001	Organic
L. Diederich [19]	Nanost.-C film	700	75	0.003	Organic
T. Osaka [20]	Activated carbon	1000–2500	8–80	0.3–3	Organic
J. Gamby [21]	Activated carbon	1200–2315	80–125	–	Organic

This paper compares the performance of ECDL capacitors with electrodes made from CNT synthesised directly on aluminium (Al) substrate, with CNT paste electrodes and with commercial available a-C electrodes. The different electrodes are tested in an electrochemical cell (Fig. 1, bottom) by impedance spectroscopy. A significant improvement of the specific capacitance ($F\,cm^{-2}$) is found for each type of active material through an increase of the mass density ($mg\,cm^{-3}$) and thickness of the active layer. Indeed, influence of the active material thickness and density on capacitance per surface area will be critically discussed and compared to various nanostructured carbon materials. As all electrodes, in this paper, have the same geometrical surface, the capacitance per surface area gives a most representative value and also allows to extrapolate the useful surface in order to obtain the wanted capacitance. Moreover, the total surface area and the BET surface area contributing to the energy storage in the double layer can be calculated from the specific capacitance ($F\,cm^{-2}$). The average capacitance per volume ($F\,cm^{-3}$) and per unit weight ($F\,g^{-1}$) values are also discussed and compared according to the physical properties of each type of active material.

2. Experimental

2.1. Types of active material

Various types of CNT and a-C have been tested as active material for ECDL capacitors (Table 3); MWNT grown in a CVD system [22], MWNT grown in a fluidised-bed CVD system [23] and commercially available a-C. The electrodes A_1 to A_3 (Table 3) consist of CVD CNT directly grown on the Al foil support [24]. The electrodes B_1 to B_4 (Table 3) consist of a paste of MWNT produced by CVD [22]. The active material of the electrodes C_1 to C_4 and D_1 to D_4 (Table 3) consist of a paste of MWNT from the fluidised-bed method. Fig. 2 shows CNT synthesised directly on Al foil support in a CVD process (Fig. 2a), paste of CNT that are produced in a fluidised-bed synthesis (Figs. 2b-c) and commercially available a-C (Fig. 2d). The CNT paste is prepared by blending mixture of 19% CNT, 24% binder solution (carboxymethylcellulose (CMC) and distilled water), 29% of methanol and 28% of water. The whole mixture is then spread on aluminium substrates.

Electrodes E_1 to E_6 use commercially available a-C material, as a reference. The a-C electrodes contain activated carbon belonging to the same supplier. They are made with various conditions in order to obtain active layer with a well-defined sticking and cohesiveness. Of the different forms of carbon, a-C is particularly attractive as an ECDL electrode because of its low cost, high specific surface area of about $1000\,m^2\,g^{-1}$ and optimum density per surface area. The physical characteristics of the various active materials were measured and are compared in Table 3.

Table 3
Physical characteristics of the different electrodes; BET surface area, thickness and density of the active material

Type of active material	BET surface area ($m^2\,g^{-1}$)	Active material thickness (μm)	Active material density ($mg\,cm^{-2}$)
A_1 (CVD CNT)	47	15	0.1
A_2 (CVD CNT)	64	25	0.27
A_3 (CVD CNT)	64	30	0.32
B_1 (CVD CNT paste)	57	50	4.45
B_2 (CVD CNT paste)	57	75	6.05
B_3 (CVD CNT paste)	57	100	7.64
B_4 (CVD CNT paste)	57	150	9.87
C_1 (fb-CNT paste)	912	50	2.1
C_2 (fb-CNT paste)	912	100	2.83
C_3 (fb-CNT paste)	912	150	4
C_4 (fb-CNT paste)	912	200	4.33
D_1 (fb-CNT paste)	120	60	5.3
D_2 (fb-CNT paste)	220	50	2
D_3 (fb-CNT paste)	370	75	5.2
D_4 (fb-CNT paste)	1064	100	1.6
E_1 (a-C)	977	100	6
E_2 (a-C)	1014	150	9.1
E_3 (a-C)	682	200	14
E_4 (a-C)	919	400	26
E_5 (a-C)	1228	600	37
E_6 (a-C)	1256	800	52

2.2. ECDL capacitors principles

The aluminium current collector and the active material make up the electrodes. The electrodes capacitance C_{cell} was measured by making an ECDL cell (Fig. 1, bottom). This consists of two gold contacts on the active material electrodes ($S = 3.14\,cm^2$). A porous membrane separator prevents electronic contact between the two electrodes. Both the separator and the electrodes are pressed and then impregnated with the organic electrolyte that is consisted of 1 M of tetraethylammonium tetrafluoroborate (Et_4NBF_4) mixed in acetonitrile (AC). The capacitance is derived from the measured impedance using Eq. (3):

$$C_{cell} = -\frac{1}{2\pi f(-\mathrm{Im}Z)} \quad (3)$$

where f is the frequency. The capacitance C_{cell} was measured by an ac-impedance spectroscopy method using a Solartron model 1186 electrochemical interface potentiostat/galvanostat and a Solartron model 1170 frequency response analyzer. The measurements were carried out at a dc bias 0 V with sinusoidal signal of amplitude 15 mV signal over the frequency range of 1 kHz to 1 mHz.

The specific double-layer capacitance CD arises from the ionic double layer at the electrode/solution interface. The diffused ions of opposite charge can be either solvated Et_4N^+ or BF_4^-. CD is calculated from Eq. (1). As the relative permittivity of the electrolyte ε_r is 40 and the diameter of the solvated ions is about 12 Å [7], CD reaches a value

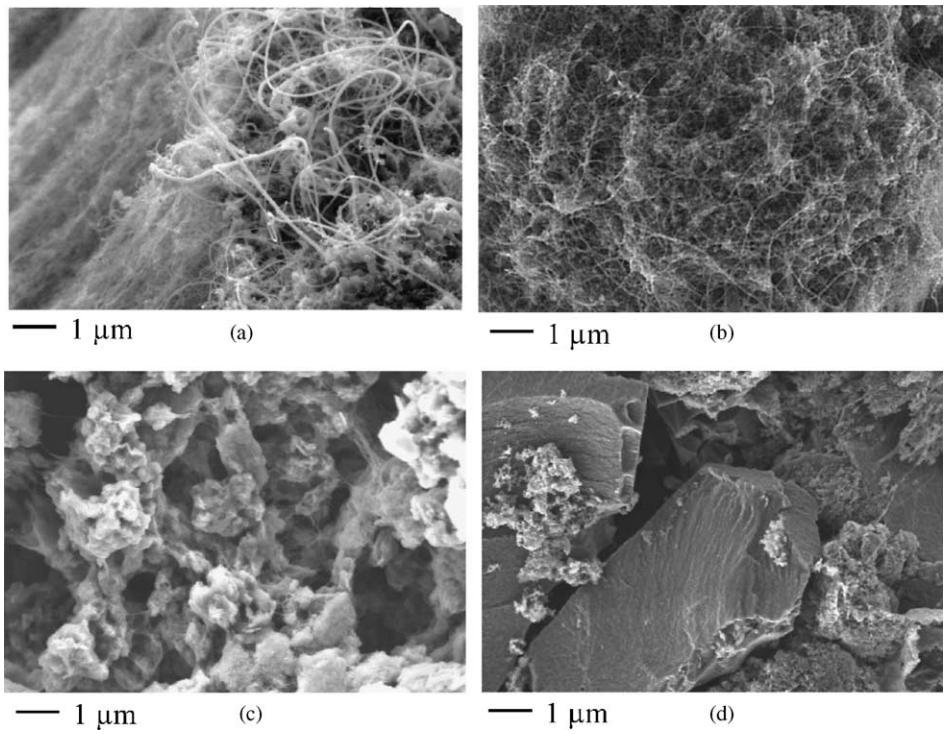

Fig. 2. SEM pictures of the various active material surface: (a) CNT synthesised in the CVD system (electrode B_2), (b) paste of MWNT ($912\,m^2\,g^{-1}$) from the fluidised-bed method (electrode C_4), (c) paste of MWNT ($220\,m^2\,g^{-1}$) synthesised in the fluidised-bed system (electrode D_2) and (d) a-C material (electrode E_3).

of $62\,\mu F\,cm^{-2}$. The theoretical specific capacitance per unit weight ($F\,g^{-1}$) can be obtained from BET surface area and CD. With Eq. (3) and assuming that m is the active material amount in one electrode, the specific capacitance C_{sp} is calculated with Eqs. (4) and (5):

$$C_{sp}\,[F\,cm^{-2}] = \frac{2C_{cell}}{A_E} \tag{4}$$

$$C_{sp}\,[F\,g^{-1}] = \frac{2C_{cell}}{m} \tag{5}$$

with A_E defined in Eq. (1).

We have developed a model to calculate the total surface area of active material A_{tot} (6) in contact with the solvated ions. We assumed that the active layer consists of pores of diameter $2d_D$ and a length d (Fig. 3). If the solvated ions have a diameter d_D and they soak into the pores, a monolayer forms in contact with active material. Eq. (6) then gives A_{tot}:

$$A_{tot}\,(cm^2) = \frac{10^4 A_E d}{(1/\rho S) + 2d_D} \tag{6}$$

Here, S ($m^2\,g^{-1}$) is the BET surface area of the active material and ρ ($g\,cm^{-3}$) is the mass density of the active material. The maximum theoretical specific capacitance C_{th} (Eq. (7)) is then derived from Eq. (6) and C_D.

$$C_{th}\,(F\,cm^{-2}) = C_D\frac{A_{tot}}{A_E} \tag{7}$$

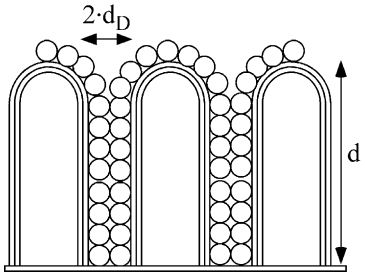

Fig. 3. Schematic view of the model to calculate (Eq. (6)) the optimal total surface area in contact with the solvated ions (○).

3. Results and discussion

The various electrodes materials give rise to different values of capacitance due to their physical characteristics (Table 3) and their morphology (Fig. 2). The specific capacitance ($F\,cm^{-2}$) in Eq. (4) gives the representative value of the storage capacity of the various materials. Indeed, the capacitance per unit weight ($F\,g^{-1}$) from Eq. (5) reaches high values, due to low mass density and low measured cell capacitance of the active materials. However, these results are not so significant and can be misleading. The active material mass density ($g\,cm^{-3}$) is calculated (Table 4) from the active layer thickness and density per surface area (Table 3).

A large increase of capacitance was obtained by increasing the thickness of the active material (Fig. 4). Kötz and

Table 4
Mass density ($g\,cm^{-3}$), average capacitance per mass ($F\,g^{-1}$) and per volume ($F\,cm^{-3}$) of the various electrodes used as ECDL capacitor

Type of electrodes	ρ ($g\,cm^{-3}$)	C ($F\,cm^{-3}$)	C ($F\,g^{-1}$)
A (CVD CNT)	0.1	1.1	12
B (CVD CNT paste)	0.78	8	10
C (fb-CNT paste)	0.29	16	76
D_1 (fb-CNT paste)	0.9	–	21 (cf. Eq. (6))
D_2 (fb-CNT paste)	0.8	–	16 (cf. Eq. (6))
D_3 (fb-CNT paste)	0.7	–	26 (cf. Eq. (6))
D_4 (fb-CNT paste)	0.16	–	79 (cf. Eq. (6))
E (a-C)	0.6	40	66

Carlen [5] describes theoretically the effect of active layer thickness by demonstrating that a thicker active layer gives a higher capacitance. Indeed, our model above shows that the specific capacitance per surface area is directly proportional to the thickness of the active layer. Indeed, in our study, the specific capacitance per surface area of the various electrodes (A to C, and E) increases linearly with the active material thickness and the density per surface area, respectively. We showed that the electrodes A with directly grown CNT are not such promising materials for the ECDL capacitors. This is because of their limited capacitance. The CNT film grown on the aluminium substrate reach a maximum thickness of 30 μm, and this can not be increased by a longer deposition time of higher precursor concentration [22]. The electrodes A show a maximum specific capacitance of $4\,mF\,cm^{-2}$. Their capacitance per volume is about $1.1\,F\,cm^{-3}$ due to the small active layer thickness and mass density. The capacitance per unit weight from Eq. (5) is about $12\,F\,g^{-1}$.

A much thicker active layer can be obtained by using a paste of CNT as active material. This greatly increases the amount of active layer contributing to the energy storage and the capacitance. Electrodes B were made of CNT produced in the same conditions as those of the electrodes A. The electrodes B (○) show a maximum specific capacitance per surface area of $0.09\,F\,cm^{-2}$ (Fig. 4). Using the linear dependence of the specific capacitance on the active material thickness (Fig. 4) and on density (Fig. 5), the average specific capacitance per volume and per unit weight (Table 4) reaches $8\,F\,cm^{-3}$ and $10\,F\,g^{-1}$, respectively. The difference of the specific capacitance per volume between the electrodes A and B is due to the eight times large mass density of the active layer of electrodes B than electrodes A (Table 4). Recently, Chen et al. [16] made electrodes based on CVD-CNT and obtained a specific capacitance of $0.05\,F\,cm^{-2}$, while Shiraishi et al. [18] achieved $10\,\mu F\,cm^{-2}$ for SWNT electrodes (Table 2). Frackowiak et al. [17] found a specific capacitance of $0.26\,F\,cm^{-2}$ for CVD MWNT electrodes.

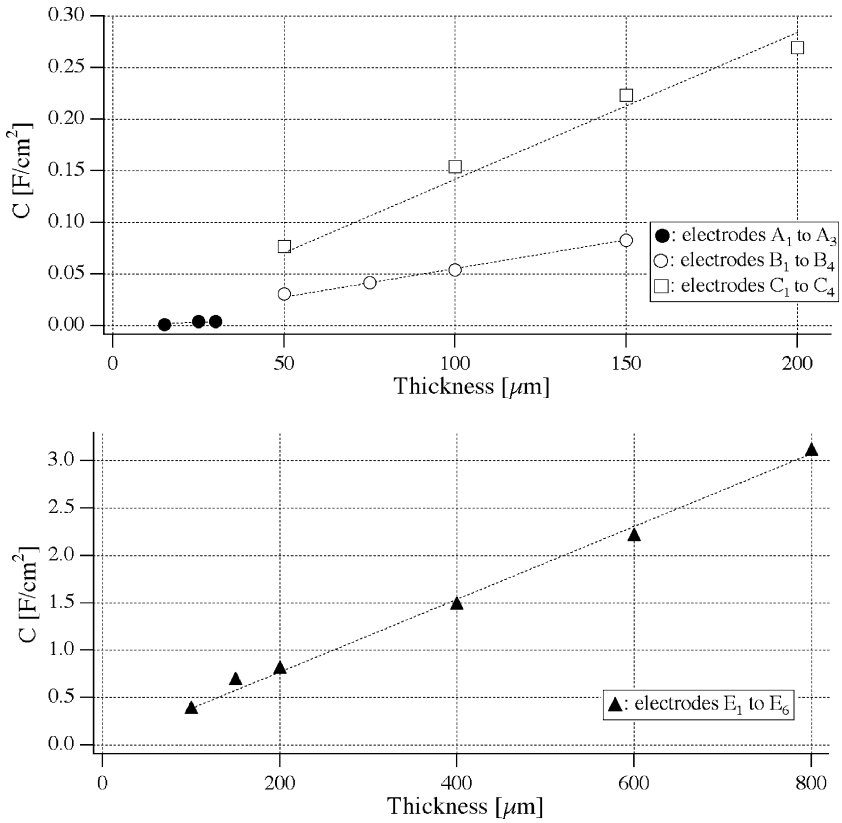

Fig. 4. Specific capacitance ($F\,cm^{-2}$) vs. thickness of active layer: (top) MWNT, (bottom) a-C.

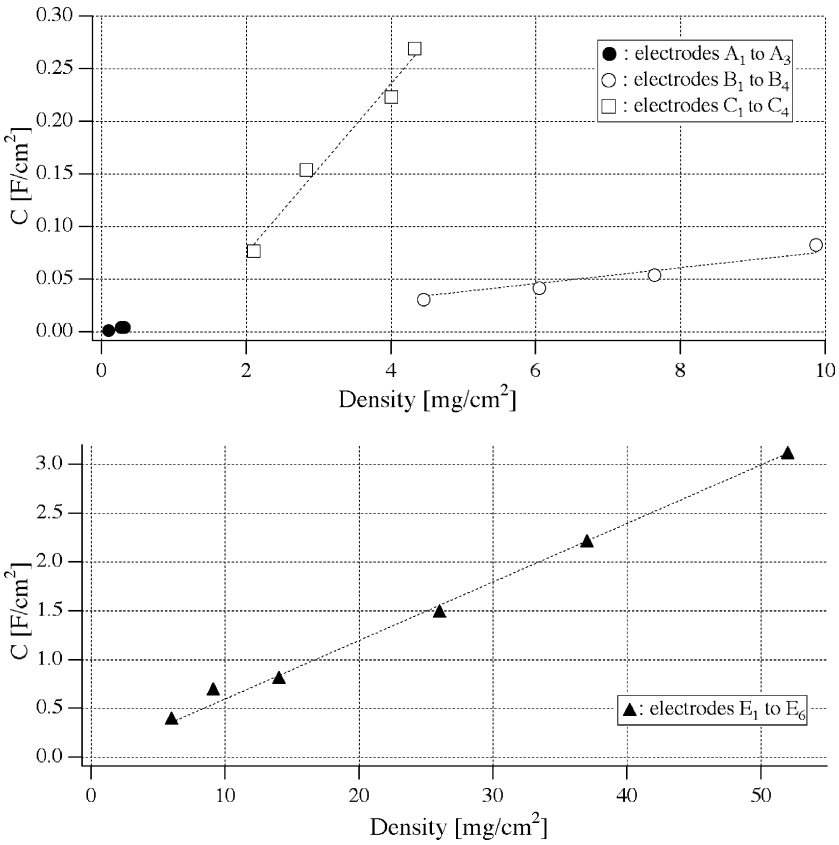

Fig. 5. Specific capacitance ($F\,cm^{-2}$) vs. density ($mg\,cm^{-2}$) of active layer: (top) MWNT, (bottom) a-C.

These results show that the capacitance of CNT-based electrodes can be increased by increasing the mass density and the active layer thickness, respectively. However, the specific capacitance can be improved by increasing the BET surface area. Indeed, the electrodes C (□) with an active layer thickness of 50 μm obtained a specific capacitance of $0.08\,F\,cm^{-2}$, and with an active layer thickness of 200 μm (Tables 3 and 4) the electrodes C (□) achieved a maximum specific capacitance of $0.27\,F\,cm^{-2}$. The average specific capacitances per volume of $16\,F\,cm^{-3}$ and per mass of $76\,F\,g^{-1}$ were derived from the slope of Figs. 4 and 5. The CNT produced in the fluidised-bed synthesis (Fig. 2b) are single-wall or double-walled CNT [23] with a BET surface area of $912\,m^2\,g^{-1}$. The small diameter pore size (8–10 nm) [23,24] and the high purity (∼98%) [22] of the fluidised-bed synthesis CNT improve greatly the access of the solvated ions in these electrodes.

The active material of the electrodes C offers a smaller accessible volume for the diffused solvated ions due to its relative small average mass density of $0.29\,g\,cm^{-3}$ (Table 4). Indeed, we observed also that the larger mass density leads to a higher capacitance. The larger density per surface area and mass density of a-C electrodes gives a greater material volume, which allows easier transport of the solvated ions from the electrolyte to the charged interface. Indeed, the electrodes E (▲) with a similar BET surface area of $1000\,m^2\,g^{-1}$ but with twice as large mass density than electrodes C (□) gives an average specific capacitance per volume of $40\,F\,cm^{-3}$ (Table 4).

The accessibility to the active layer depends on the diffusion of solvated ions and more precisely of the pores distribution, which seems to be influenced by the mass density. The performance characteristics of ECDL capacitors differ somewhat from those of conventional capacitors. While the ideal capacitor shows a vertical slope of the imaginary part, the ECDL capacitors starts with a 45° impedance line and approaching an almost vertical slope only at low frequencies. The non-vertical slope of the low frequency impedance of any real ECDL capacitor is a typical feature of electrochemical charging processes, and may be interpreted as resulting from a distribution in non-uniform active layer [25] or a distribution in microscopic charge transfer rates [26], adsorption processes, or surface roughness. The 45° region known as Warburg region is a consequence of the distributed resistance/capacitance in a porous electrode. De Levie [27] and Song et al. [28] have given a complete theoretical description of the porous electrode behaviour and they demonstrated that an increase of the active layer thickness with constant pores radius results to an increase of the Warburg region that leads to a higher capacitance. The Nyquist plot in Fig. 6 shows a region at high frequency of 45° slope that is explained as arising from the diffusion of

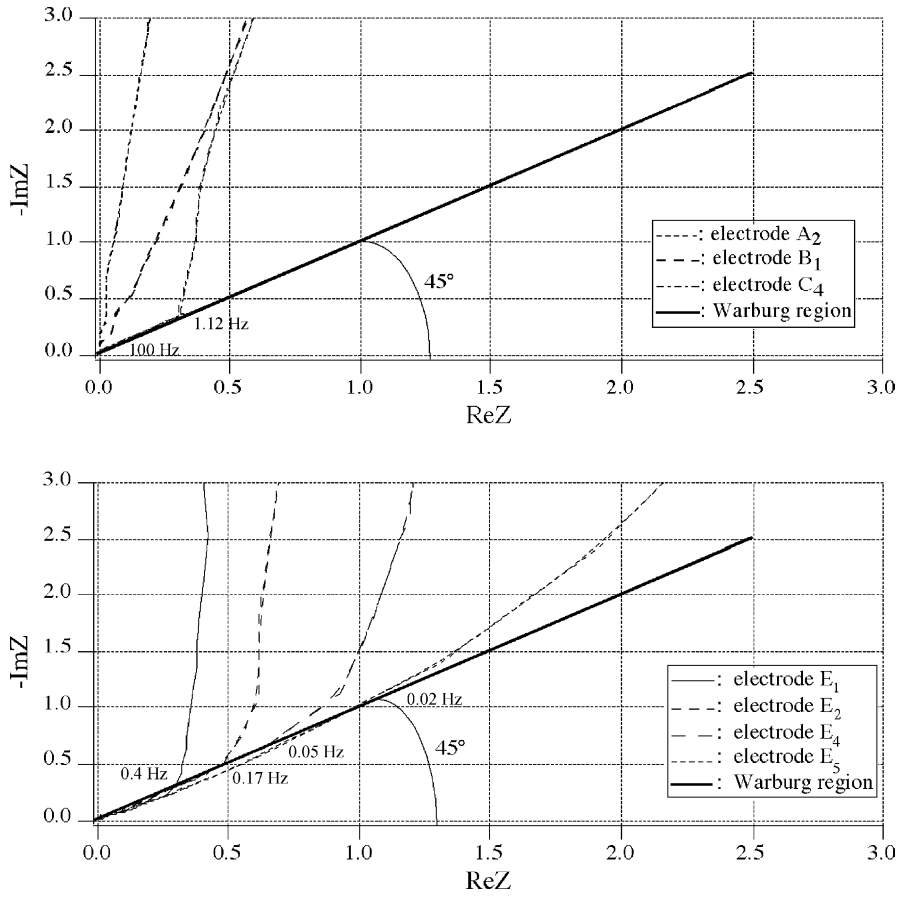

Fig. 6. Nyquist impedance plot in the Warburg region for: (top) CNT electrodes, (bottom) a-C electrodes.

ions at high frequency in the active material. The vertical slope of the imaginary part in the lower frequencies corresponds then to a pure capacitance. The Nyquist impedance plot (Fig. 6) in the Warburg region for the CNT electrodes shows a weak ions diffusion (Fig. 6, top), while the diffusion region is quite significant for electrodes E (Fig. 6, bottom).

We established that the volume accessibility is associated with the active material thickness and particularly with the mass density, but less with the BET surface area. Indeed, the specific surface area corresponds to the area accessible for the gas (N_2) adsorption [29] in the micropores (diameter <20 Å). According to the theoretical relation of Niu et al. [13], the theoretical specific capacitance per unit weight would be C (F g^{-1}) $= C_D$BET (cf. Chapter 2.2) increasing linearly with the BET surface area. However, our measurements show that the specific capacitance per unit weight is not linearly dependent on the BET surface area. Indeed, for the highest values of the specific surface area, an important fraction of electrolyte cannot penetrate in the active layer volume due to small pore sizes. The size of the solvated ions limits the transport to the largest pores [7]. Micropores in the active layer are not accessible to the solvated ions and they do not contribute to energy storage. Hence, the BET area is not sufficient to predict the ionic adsorption and the specific capacitance (F g^{-1}).

The behaviour of the specific capacitance per surface area according to the BET surface area is also complex. Indeed, the normalised specific capacitance per surface area can be plotted with Eq. (7) (Fig. 7) by using an active layer thickness of the CNT and a-C electrodes of 100 μm. Using values from Tables 3 and 4, we estimate the maximum average pore diameter D (Eq. (6)) of the CNT electrodes to be 400–420 Å (Fig. 7, top), and 100–120 Å for electrodes E from (Fig. 7, bottom). Electrodes E have a more efficient volume accessibility and a larger specific capacitance per surface area due to their larger mass density.

Various methods were used to increase the specific capacitance. Recently, Endo et al. [30] developed ECDL capacitors based on activated carbon by mixing CVD carbon fibre as an additive. A maximum specific capacitance of 12 F cm^{-3} was achieved without increasing the active layer thickness.

The active material of the electrodes E shows efficient physical properties (Tables 3 and 4) as larger thickness and density (mg cm^{-2}) and especially an optimum average pore diameter, which allows an easier access of ions into the active material volume. The Warburg region study on the Nyquist plot confirms clearly these results.

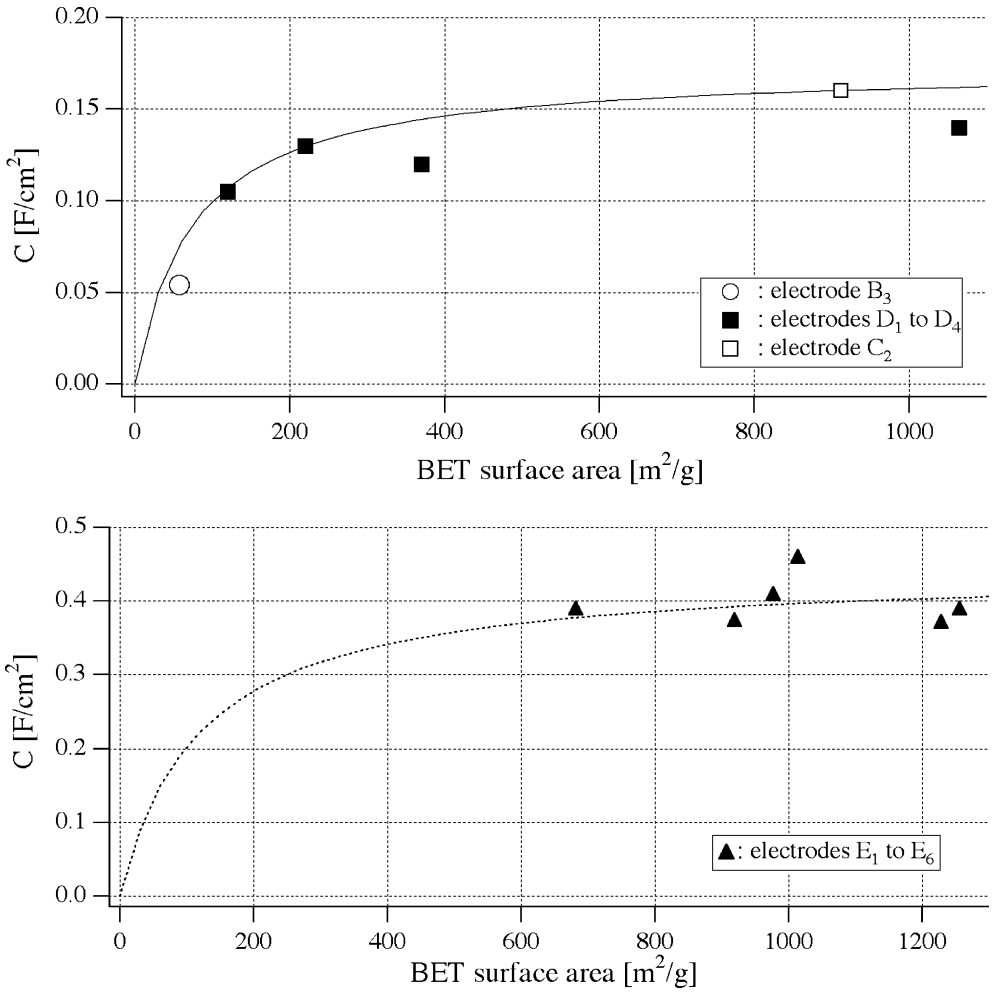

Fig. 7. Specific capacitance (F cm^{-2}) vs. BET surface area plotted from Eq. (2): (top) MWNT, (bottom) a-C. The specific capacitance is normalised to an active material thickness of 100 μm.

4. Conclusion

Active materials used for the ECDL capacitors have to develop high specific capacitance per surface area and per volume. Various electrodes based on CNT and a-C were studied. An increase of the specific capacitance per surface area was achieved by increasing the active layer thickness and particularly the mass density. The ECDL capacitors using CNT reached a specific capacitance of 0.8–280 mF cm^{-2} and 1.1–16 F cm^{-3}, respectively. As the CNT films produced by CVD have a maximum thickness of 30 μm, the electrodes A do not make efficient ECDL capacitors.

Due to their high gravimetric density, the activated carbon (electrodes E) showed a large accessible volume for the diffusion of solvated ions and thus a high specific capacitance. The electrochemical impedance spectroscopy measurements of the electrodes E showed a significant Warburg region, which confirmed the efficient ions diffusion in the bulk of the active layer. This shows that the activated carbon electrodes E are a promising material for ECDL capacitors, with specific capacitance ranging from 0.4 to 3.1 F cm^{-2}. Because of their large mass density, they reach an average specific capacitance of 40 F cm^{-3} and 66 F g^{-1}, respectively.

Improving the CNT electrodes capacitance would be possible by increasing the mass density of the active material, for example by modifying the mixture in the CNT paste. Like this, due to their production simplicity and their physical properties the CNT electrodes can replace the a-C as ECDL in the near future. Meanwhile, our investigations demonstrated that the more suitable active material for the ECDL applications has to be composed of large mass density and thick films.

Acknowledgements

We would like to thank the *Paul Scherrer Institute* for producing the CNT paste electrodes (electrodes C2 to C4), the *Centre Interdépartemental de Microscopie Electronique* of the *Ecole Polytechnique Fédérale de Lausanne* for

access to scanning electron microscopes and more particularly J.-M. Bonard (EPFL-CH) for his collaboration. The OFES is acknowledged for the financial support of the "Carben" EU-project.

References

[1] T. Christen, M.W. Carlen, J. Power Source 91 (2000) 210.
[2] M. Endo, T. Takeda, Y.J. Kim, K. Koshiba, K. Ishii, Carbon Sci. 1 (2001) 117.
[3] A. Schneuwly, P. Gröning, L. Schlapbach, P. Brüesch, M.W. Carlen, R. Gallay, Mater. Sci. Eng. B54 (1998) 182.
[4] A. Schneuwly, A. Züttel, Ch. Emmenegger, V. Härri, R. Gallay, Proc. Power Conv. PCIM (1999).
[5] R. Kötz, M. Carlen, Electrochim. Acta 45 (2000) 2483.
[6] H.L.F. Helmholtz, Ann. Phys. 89 (1879) 211.
[7] M. Ue, Curr. Topics Electrochem. 7 (2000) 49.
[8] S. Iijima, Nature 354 (1991) 56.
[9] E. Frackowiak, F. Béguin, Carbon 39 (2001) 937.
[10] S. Brunauer, P.H. Emmet, E. Teller, J. Am. Chem. Soc. 60 (1938) 309.
[11] P. Bernier, W. Maser, C. Journet, A. Loiseau, M.L. de la Chapelle, S. Lefrant, R. Lee, J.E. Fischer, Carbon 36 (1998) 675.
[12] A. Burke, J. Power Source 91 (2000) 37.
[13] Ch. Niu, E.K. Sichel, R. Hoch, D. Moy, H. Tennent, Appl. Phys. Lett. 70 (1997) 1480.
[14] K.H. An, W.S. Kim, Y.S. Park, Y.C. Choi, S.M. Lee, D.C. Chung, D.J. Bae, S.C. Lim, Y.H. Lee, Adv. Mater. 13 (2001) 497.
[15] R.Z. Ma, J. Liang, B.Q. Wei, B. Zhang, C.L. Xu, D.H. Wu, J. Power Sources 84 (1999) 126.
[16] J.H. Chen, W.Z. Li, D.Z. Wang, S.X. Yang, J.G. Wen, Z.F. Ren, Carbon 40 (2002) 1193.
[17] E. Frackowiak, K. Jurewicz, S. Depleux, F. Beguin, J. Power Source 97/98 (2001) 822.
[18] S. Shiraishi, H. Kurihara, K. Okabe, D. Hulicova, A. Oya, Electrochem. Commun. 4 (2002) 593.
[19] L. Diederich, E. Barborini, P. Piseri, A. Podesta, P. Milani, A. Schneuwly, R. Gallay, Appl. Phys. Lett. 75 (1999) 2662.
[20] T. Osaka, X. Liu, M. Nojima, T. Momma, J. Electrochem. Soc. 146 (1999) 1724.
[21] J. Gamby, P.L. Taberna, P. Simon, J.F. Fauvarque, M. Chesneau, J. Power Source 101 (2001) 109.
[22] Ch. Emmenegger, J.-M. Bonard, Ph. Mauron, A. Züttel, P. Sudan, A. Lepora, B. Grobety, L. Schlapbach, Carbon 41 (2003) 539.
[23] Ph. Mauron, Ch. Emmenegger, P. Sudan, P. Wenger, S. Rentsch, A. Züttel, in: T.S. Srivatsan, R.A. Varin (Eds.), Proceedings of the 11th International Symposium on Processing and Fabrication of Advanced Materials, vol. 8, Columbus, OH, USA, 2002.
[24] Ch. Emmenegger, Ph. Mauron, P. Sudan, P. Wenger, V. Hermann, R. Gallay, A. Züttel, in: T.S. Srivatsan, R.A. Varin (Eds.), Proceedings of the 11th International Symposium on Processing and Fabrication of Advanced Materials, vol. 8, Columbus, OH, USA, 2002.
[25] M.F. Mathias, O. Haas, J. Phys. Chem. 97 (1993) 9217.
[26] H. Scher, M. Lax, Phys. Rev. B7 (1973) 4491.
[27] R. De Levie, in: P. Delahay (Ed.), Advances in Electrochemistry and Electrochemical Engineering, vol. 6, Interscience, New York, 1967, p. 329.
[28] H.K. Song, H.Y. Hwang, K.H. Lee, L.H. Dao, Electrochim. Acta 45 (2000) 2241.
[29] A. Züttel, P. Sudan, Ph. Mauron, T. Kiyobayashi, Ch. Emmenegger, L. Schlapbach, J. Hydrogen Energy 27 (2002) 203.
[30] M. Endo, T. Takeda, Y.J. Kim, K. Koshiba, K. Ishii, Carbon Sci. 1 (3/4) (2001) 117.